J Biomol NMR (2015) 63:367–373
DOI 10.1007/s10858-015-9995-7

ARTICLE

Extracting protein dynamics information from overlapped NMR signals using relaxation dispersion difference NMR spectroscopy

Tsuyoshi Konuma[1,2] · Erisa Harada[1] · Kenji Sugase[1,3]

Received: 8 June 2015 / Accepted: 14 October 2015 / Published online: 17 October 2015

Abstract Protein dynamics plays important roles in many biological events, such as ligand binding and enzyme reactions. NMR is mostly used for investigating such protein dynamics in a site-specific manner. Recently, NMR has been actively applied to large proteins and intrinsically disordered proteins, which are attractive research targets. However, signal overlap, which is often observed for such proteins, hampers accurate analysis of NMR data. In this study, we have developed a new methodology called relaxation dispersion difference that can extract conformational exchange parameters from overlapped NMR signals measured using relaxation dispersion spectroscopy. In relaxation dispersion measurements, the signal intensities of fluctuating residues vary according to the Carr-Purcell-Meiboon-Gill pulsing interval, whereas those of non-fluctuating residues are constant. Therefore, subtraction of each relaxation dispersion spectrum from that with the highest signal intensities, measured at the shortest pulsing interval, leaves only the signals of the fluctuating residues. This is the principle of the relaxation dispersion difference method. This new method enabled us to extract exchange parameters from overlapped signals of heme oxygenase-1, which is a relatively large protein. The results indicate that the structural flexibility of a kink in the heme-binding site is important for efficient heme binding. Relaxation dispersion difference requires neither selectively labeled samples nor modification of pulse programs; thus it will have wide applications in protein dynamics analysis.

Keywords Protein dynamics · Relaxation dispersion difference · Overlapped signal · Heme oxygenase-1

Introduction

Protein structures are not static, but rather they dynamically fluctuate to exert their function. Recent advances in experimental methodologies have provided important insights into the relationship between the dynamics and function of various proteins. For example, protein dynamics play a central role in enzyme catalysis involving substrate binding and product release (Bhabha et al. 2011; Nashine et al. 2010). Of the methodologies applied, Carr–Purcell–Meiboom–Gill (CPMG) relaxation dispersion (RD) NMR spectroscopy is one of the most powerful techniques for quantitating protein dynamics (Loria et al. 1999a; Tollinger et al. 2001), being able to analyze site-specific conformational exchange of a protein on the millisecond time scale. This time scale is relevant to numerous important biological processes, such as protein–protein interactions (Sugase et al. 2007a, b; Vallurupalli et al. 2008), protein folding (Meinhold and Wright 2011), and enzyme catalysis (Bhabha et al. 2011; Boehr et al. 2006b; Henzler-Wildman et al. 2007). It can also provide

Electronic supplementary material The online version of this article (doi:10.1007/s10858-015-9995-7) contains supplementary material, which is available to authorized users.

✉ Kenji Sugase
sugase@sunbor.or.jp; sugase@moleng.kyoto-u.ac.jp

[1] Bioorganic Research Institute, Suntory Foundation for Life Sciences, 1-1-1 Wakayamadai, Shimamoto, Mishima, Osaka 618-8503, Japan

[2] Present Address: Department of Structural and Chemical Biology, Icahn School of Medicine at Mount Sinai, New York, NY 10029, USA

[3] Present Address: Department of Molecular Engineering, Graduate School of Engineering, Kyoto University, Kyoto-Daigaku Katsura, Nishikyo-Ku, Kyoto 615-8510, Japan

structural information on low-populated states, which are invisible to most biophysical methods, in the form of chemical shift differences between interconverting states of proteins.

RD experiments require accurate quantification of signal intensities, which are converted to effective transverse relaxation rates, R_2^{eff}. It is a prerequisite that isolated signals are observable in the RD experiments. However, NMR signals of large proteins and intrinsically disordered proteins (IDPs) tend to be overlapped because of a large number of signals and/or poor signal dispersion. Although these proteins are attractive targets for dynamics studies, such signal overlaps hamper accurate analysis of RD data. Indeed, we encountered this problem of signal overlap while we were analyzing RD data from heme oxygenase-1 (HO-1), which is a relatively large protein composed of 232 residues (Harada et al. 2015b). One solution to this kind of problem is selective isotope labeling of residues of interest. However, obtainable information is reduced, and thus multiple NMR samples that are differently isotope-labeled may be prepared to obtain the whole picture of dynamics of a protein. Preparation of multiple samples and conducting NMR experiments is time-consuming. Moreover, selective isotope labeling requires isotope labeled compounds that are more expensive than uniform labeling. Therefore, an alternative solution is desired. In this article, we describe a newly developed methodology called relaxation dispersion difference (RDD) NMR spectroscopy that can extract protein dynamics information from overlapped NMR signals of a uniformly labeled sample.

Materials and methods

Theory

In the case of R_1, R_2, $R_{1\rho}$, and NOE measurements, all signals (except for those of side chains in ^{15}N relaxation experiments) are used for analyzing protein dynamics unless the signals are overlapped. In contrast, not all signals in RD experiments provide meaningful protein dynamics information because the RD method was developed to quantitate the excess contribution to the effective transverse relaxation rate, R_{ex}, which is usually caused by a relatively large conformational fluctuation localized to a specific region in a protein, for example, a ligand-binding site. Therefore, only signals of fluctuating residues that have R_{ex} are used for the analysis, whereas those of non-fluctuating residues that have no R_{ex} provide no protein dynamics information, and are thus discarded in the RD analysis. In many cases, useless signals from non-fluctuating residues overlap with those of fluctuating residues. Therefore, if the signals of non-fluctuating residues are removed from the spectra, the fluctuation of the residues can be quantitatively analyzed.

To achieve this in RDD experiments, R_2^{eff} is measured using the conventional RD pulse sequence with no modification (Loria et al. 1999a, b; Tollinger et al. 2001), and then difference spectra are calculated according to Eq. (1):

$$\Delta I(\tau_{\mathrm{CP}}) = I(0)\left\{\exp\left[-R_2^{\mathrm{eff}}(\tau_{\mathrm{CP}}^{\mathrm{min}})T_{\mathrm{CPMG}}\right] - \exp\left[-R_2^{\mathrm{eff}}(\tau_{\mathrm{CP}})T_{\mathrm{CPMG}}\right]\right\}, \quad (1)$$

where $I(0)$ represents the signal intensity in the reference spectrum acquired by omitting the constant CPMG period, T_{CPMG}. τ_{CP} is the CPMG pulsing interval, and $\tau_{\mathrm{CP}}^{\mathrm{min}}$ is the shortest τ_{CP} among a series of RD measurements at which R_{ex} is most suppressed. $\Delta I(\tau_{\mathrm{CP}})$ of fluctuating residues varies according to τ_{CP} in an RDD profile (Fig. 1a), whereas those of non-fluctuating residues stay constant over all τ_{CP}, and thus $\Delta I(\tau_{\mathrm{CP}})$ of non-fluctuating residues is as low as the baseline (Fig. 1b). Thus, the spectral subtraction leaves only signals of the fluctuating residues in the difference spectra. In practice, the subtraction is executed for the free induction decay (FID), and $\Delta I(\tau_{\mathrm{CP}})$ is obtained from the difference spectra after Fourier transformation. Note that $I(0)$ cannot precisely be quantitated from overlapped signals in the reference spectrum. Therefore, RDD data are recorded for at least three different T_{CPMG}, and are fitted simultaneously with $I(0)$ being treated as a fitting parameter.

NMR measurements

NMR experiments were performed on AVANCE DRX600 and AVANCE DMX750 (Bruker BioSpin) at 293 K using 0.5 mM uniformly ^{2}H/^{15}N-labeled rat HO-1 (residues 1-232) dissolved in 50 mM potassium phosphate (pH 7.0) containing 5 % D_2O. The protein preparation and chemical shifts assignments have been previously described (Harada et al. 2015a, b). ^{15}N R_2 relaxation rates were measured using the TROSY-type constant-time CPMG pulse sequence with relaxation delays of $T_{\mathrm{CPMG}} = 20$, 40, and 80 ms (Loria et al. 1999a). Two-dimensional data sets with 512×128 ($t_2 \times t_1$) complex points were acquired at $\tau_{\mathrm{CP}} = 10$, 5, 3.33, 2.5, 2.0, 1.66, 1.43, 1.25, 1.0, 0.83, 0.71, 0.63, 0.55, 0.50, 0.4, and 0.33 ms.

RDD processing and data analysis

To obtain RDD spectra, the spectral subtraction was performed for FID by executing the "addNMR-sub" command, which is included in the NMRPipe system (Delaglio et al. 1995), and then Fourier transformation was applied to the subtracted FID. Signal picking was performed using the

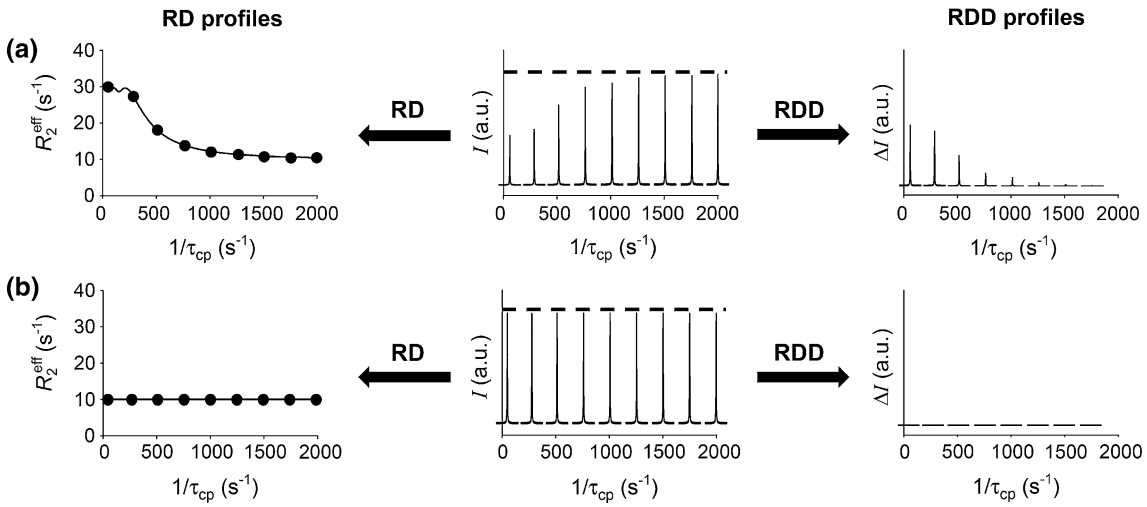

Fig. 1 Principle of RDD. **a** RD and RDD profiles of fluctuating residues. Each intensity (*middle*) is converted to the effective transverse relaxation rate for RD (*left*), and is subtracted from the one measured at the largest $1/\tau_{CP}$ for RDD (*right*). The *dashed line* in the *middle figure* represents the highest intensity measured at the largest $1/\tau_{CP}$. (b) RD and RDD profiles of non-fluctuating residues. RD and RDD profiles are created in the same manner as in (**a**). The difference spectra provide constant intensities, equivalent to the baseline, in the RDD profile

NMRView program (Johnson and Blevins 1994). For the calculation of R_2^{eff} in Eq. (1), we used the Carver and Richards equation (Carver and Richards 1972), which calculates well-approximated R_2^{eff} for all exchange regimes of a two-state conformational exchange model (A $\leftrightarrow$ B). The fitting was performed using the GLOVE program with global parameters of k_{ex} and $p_{\mathrm{A}}p_{\mathrm{B}}$ and local parameters of $|\Delta\omega|$ and R_2^0 (Sugase et al. 2013). $I(0)$ is also used as a fitting parameter in the case of the RDD method.

Results and discussion

Initially, we validated the RDD method using synthetic data simulated for ^{15}N magnetic fields of 60.8 and 76.0 MHz. R_2^{eff} rates were calculated for $T_{\mathrm{CPMG}} = 20$, 40, and 80 ms with a p_{B} of 0.02 and with both $\Delta\omega$ and k_{ex} ranging from 50 to 2950 (rad s^{-1} for $\Delta\omega$ and s^{-1} for k_{ex}). R_2^0 rates at 60.8 and 76.0 MHz were set to 5 and 8 s^{-1}, respectively. The calculated R_2^{eff} rates were converted to intensities, and 2 % random errors were added. The synthetic RDD data were fitted to Eq. (1), and the fitted values of $\Delta\omega$ and k_{ex} were compared to the input values (Figure S1). The coefficients of determination for $\Delta\omega$ and k_{ex} were 0.99 and 0.97, respectively, indicating that RDD is a reliable method. Note that R_2^0 determined by RDD may not be accurate because R_2^0 is included in the second term in the Taylor expansion of Eq. (1) as shown below (T_{CPMG}^2 should be a very small value), thus deviation of R_2^0 contributes little to $\Delta I(\tau_{\mathrm{CP}})$.

$$\begin{aligned}\Delta I(\tau_{\mathrm{CP}}) \approx & \left[R_2^{\mathrm{eff}}(\tau_{\mathrm{CP}}) - R_2^{\mathrm{eff}}(\tau_{\mathrm{CP}}^{\mathrm{min}})\right] T_{\mathrm{CPMG}} \\ & - \frac{1}{2}\left[R_2^{\mathrm{eff}}(\tau_{\mathrm{CP}}) + R_2^{\mathrm{eff}}(\tau_{\mathrm{CP}}^{\mathrm{min}}) + 2R_2^0\right] \\ & \times \left[R_2^{\mathrm{eff}}(\tau_{\mathrm{CP}}) - R_2^{\mathrm{eff}}(\tau_{\mathrm{CP}}^{\mathrm{min}})\right] T_{\mathrm{CPMG}}^2 + \cdots\end{aligned} \quad (2)$$

Subsequently, RDD was applied to HO-1, which degrades heme into iron, carbon monoxide, and biliverdin IXα by specifically cleaving the α-meso position of heme (Figure S2) (Kikuchi et al. 2005). Recently, we analyzed the dynamics of HO-1 in the free state using RD, and revealed that the CD loop, which is distal from the heme-binding site, remotely regulates the heme-binding process (Harada et al. 2015b). The RD experiments also showed that some residues in the F helix, which forms the heme-binding site with A and B helices, are partially unfolded in the low-populated minor state. We found that this partial unfolding of the F helix is important for efficient heme binding. However, we encountered a problem in that the RD data of Tyr137, Asp140, and Leu141 in the F helix were unable to be analyzed on account of signal overlaps (Fig. 2a; Figure S3). Asp140 and Leu141 are involved in the kink of the F helix, which largely changes conformation upon heme binding (Fig. 2b; Lad et al. 2003) and therefore, they are also likely to fluctuate in concert with the other residues in the F helix.

In the RDD experiments for HO-1, we measured TROSY-type ^{15}N relaxation dispersions (Loria et al. 1999b) with T_{CPMG} of 20, 40, and 80 ms at ^{15}N magnetic fields of 60.8 and 76.0 MHz. First, to validate the reliability of the RDD method using experimental data,

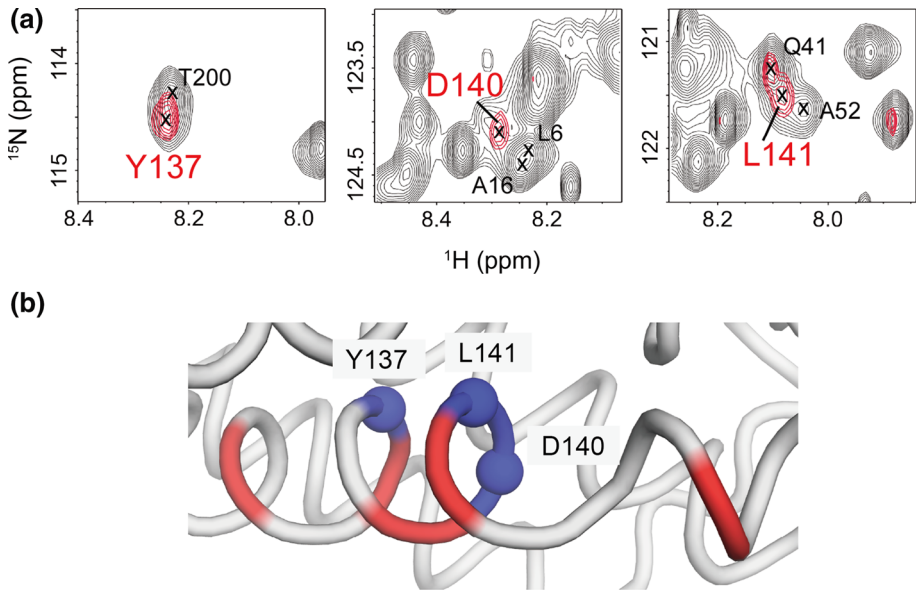

Fig. 2 **a** The reference (*black*) and difference (*red*) spectra of free HO-1 in the RDD experiment. The reference spectrum was acquired by omitting T_{CPMG}. The difference spectrum was acquired by subtracting the RD spectrum at $1/\tau_{CP}$ of 100 s^{-1} from the one at $1/\tau_{CP}$ of 3000 s^{-1}. **b** Closed view of the structure of F helix in free HO-1. Fluctuating residues analyzed by RDD and RD are colored-coded in *blue* and *red*, respectively

we analyzed six isolated signals, namely those of Tyr134, Arg136, Gly139, Ser142, Val146, and Lys153 in the F helix by both conventional RD and RDD. Note that RDD can, of course, be applied to isolated signals. In this validation, we created an RDD dataset for one out of the six residues and five RD datasets for the rest of the residues, and performed a global fit of the mixed RDD and RD datasets. The fitted results were compared to those obtained by the analysis of the six datasets using only the RD method. This process was repeated six times by changing the dataset (residue) to be analyzed using the RDD method. Here, to obtain accurate results using the RDD method, we firstly analyzed the signal intensities in the 3D HNCO spectrum of HO-1, which was used for the chemical shift assignment (Harada et al. 2015b). The signals of Tyr134, Arg136, Gly139, Ser142, V146, and Lys153 were isolated in the HNCO spectrum and their intensities were all larger than $I_{ave,HNCO}$–$I_{std,HNCO}$, where $I_{ave,HNCO}$ is the averaged intensity of all isolated resonances in the HNCO spectrum and $I_{std,HNCO}$ is its standard deviation (Figure S4). Since the signal intensities in the 3D HNCO spectrum should be nearly proportional to those in the 2D HSQC or RD spectra, we restricted the exploring space of $I(0)$ in the fitting process by setting its lower limit to $I_{ave,RD}$–$I_{std,RD}$. In this case, $I_{ave,RD}$ and $I_{std,RD}$ were calculated for the RD spectra. As a result, chemical shift differences, $\Delta\varpi$ (= $|\Delta\omega/2\pi B_0|$), derived from RDD were well correlated with those from RD (Fig. 3). The obtained global parameters k_{ex} and p_B for each RD dataset were coincident with the values determined using only RD within the error range, showing the robustness of the RDD method (Table S1).

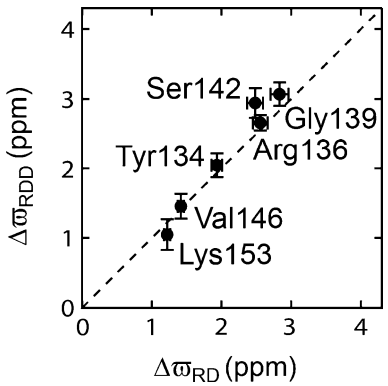

Fig. 3 Correlation between chemical shift differences obtained from the conventional RD method ($\Delta\varpi_{RD}$) and those obtained from the RDD method ($\Delta\varpi_{RDD}$). The coefficient of determination was 0.97. The *dashed line* is drawn with a slope of unity and an intercept of zero to guide the eye

Subsequently, we analyzed the signals of Tyr137, Asp140, and Leu141 in the F helix using RDD. These signals overlap with other signals, but the chemical shifts of the signals left in the subtracted spectra match those of Tyr137, Asp140 and Leu141 (Fig. 2a). The signal of Leu141 in the subtracted spectra is still partly overlapped with that of Gln41, which is also a fluctuating residue. We firstly tried to enhance the resolution of the subtracted spectra by applying several window functions. Some of them provided the completely separated signals of Leu141 and Gln41 (Figure S5), but their intensities were significantly decreased. Therefore, we adopted the window functions that moderately enhance the spectral resolution: a 9-degree shifted cosine and a squared cosine functions for

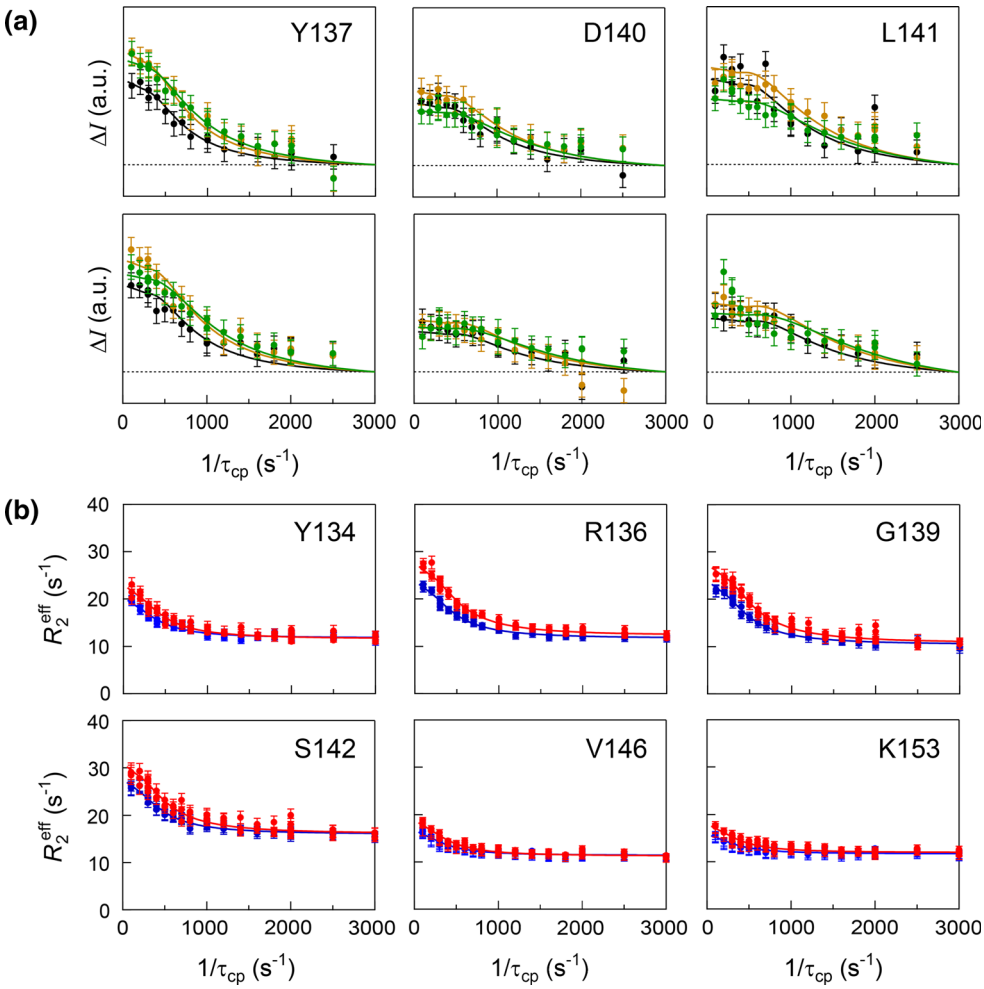

Fig. 4 **a** RDD profiles for Y137, D140, and L141 recorded with T_{CPMG} of 20 ms (*black*), 40 ms (*yellow*), and 80 ms (*green*) at ^{15}N frequencies of 60.8 MHz (*upper*) and 76.0 MH (*lower*). *Solid lines* represent the best-fitted curves to the experimental data using Eq. 1. The *dotted lines* represent an intensity of zero, corresponding to the baseline. **b** RD profiles for Y134, R136, G139, S142, V146, and K153 recorded with T_{CPMG} of 20, 40, and 80 ms at ^{15}N frequencies of 60.8 MHz (*blue*) and 76.0 MH (*red*). *Solid lines* represent the best-fitted curves to the experimental data using the Carver and Richards equation. Standard deviations of the fitting parameters were estimated by Monte Carlo simulations using 100 synthetic datasets generated on the basis of the experimental uncertainties

the F_2 (^{1}H) and F_1 (^{15}N) dimensions, respectively. Furthermore, we obtained the signal intensities only from the peak tops in the subtracted spectra. Therefore, the obtained signal intensities of interest contain no or little contribution from other unwanted signals.

The RDD profiles of Tyr137, Asp140 and Leu141, and those of Tyr134, Arg136, Gly139, Ser142, Val146 and Lys153 are shown in Fig. 4a, b, respectively. The three RDD datasets of the overlapped signals and the six RD datasets of the isolated signals were fitted globally, yielding the global parameters ($k_{ex} = 1089 \pm 42$ s^{-1} and $p_B = 2.58 \pm 0.15$ %). The global parameters and the chemical shift differences were in excellent agreement with those from the only isolated signals processed by RD ($k_{ex} = 1027 \pm 45$ s^{-1} and $p_B = 2.37 \pm 0.11$ %) (Table 1). These results again demonstrate the reliability of the RDD method.

The analyzed residues were mapped onto the crystal structure of HO-1 (Fig. 2b). The $\Delta\varpi$ values of Tyr137, Asp140 and Leu141 were relatively large compared with those of other residues in the F helix (Table 1), indicating that the three residues unfold at a larger amplitude than other residues in the F helix. This result also highlights that the structural flexibility of the kink is important for heme recognition. The structural flexibility would partially disrupt helix formation of the heme-binding F helix to

Table 1 Chemical shift differences of F-helix in HO-1

Residue	RDD + RD[a] $\Delta\varpi$[c] (ppm)	RD[b] $\Delta\varpi$[c] (ppm)
Tyr134	1.87 ± 0.07	1.93 ± 0.07
Arg136	2.45 ± 0.10	2.56 ± 0.10
Tyr137	4.41 ± 0.24	–
Gly139	2.69 ± 0.11	2.83 ± 0.13
Asp140	6.81 ± 0.49	–
Leu141	7.92 ± 0.42	–
Ser142	2.37 ± 0.09	2.48 ± 0.10
Val146	1.38 ± 0.04	1.42 ± 0.04
Lys153	1.19 ± 0.04	1.22 ± 0.04

[a] Data sets of Tyr137, Asp140, and Leu141 were analyzed by the RDD method and the others by the conventional RD method

[b] All data sets were analyzed by the conventional RD method

[c] Chemical shift differences are calculated according to the formula: $\Delta\varpi$ (ppm) = $|\Delta\omega(\text{rad s}^{-1})/2\pi B_0|$, where B_0 is the ^{15}N resonance frequency

facilitate heme insertion into the binding pocket. Previous mutagenesis studies showed that the kink is essential for heme-degradation activity (Lightning et al. 2001; Liu et al. 2000). We propose that the mutations not only alter the affinity for heme but also change the flexibility of the kink, resulting in the impaired activity. In contrast, this kink region forms a stable α-helix in the heme-bound state, and thus this helical conformation would be induced by heme binding rather than preexisting in the free state.

Spin relaxation NMR spectroscopy such as RD, ZZ-exchange, R_1, R_2, $R_{1\rho}$, and NOE experiments provide fruitful protein dynamics information (Boehr et al. 2006a), but they commonly have the signal overlap problem in accurate quantification of signal intensities. Several solutions to circumvent this problem, other than selective isotope labeling, have been reported. For example, spectral deconvolution has been utilized in R_1, R_2, and NOE experiments to resolve overlapped signals in NMR spectra (Gutmanas et al. 2004). However, it is difficult to deconvolute signals with a high degree of chemical shift degeneracy. Indeed, we were not able to obtain well-deconvoluted signals of Leu141 in the RD spectra and the resulting RD profile (Figure S3). A projection-reconstruction technique has been used for recording 2D projection planes for measurements of ^{15}N $R_{1\rho}$ relaxation rates (Tugarinov et al. 2004). This method has the benefit of introducing a third chemical shift evolution without increasing the dimensionality by simultaneous incrementation of a pair of indirect evolution delays (t_1 and t_2) in a 3D-type experiment. However, a ^{13}C- and ^{15}N-labeled sample and modification of the pulse program are required. In contrast, RDD requires only subtraction of FID. In principle, even if many signals of non-fluctuating residues overlap with that of a single fluctuating residue with a high degree of chemical shift degeneracy, RDD can extract dynamics information on the fluctuating residue. Thus, RDD is especially effective for the analyses of large proteins and IDPs because their signals are often severely overlapped. Furthermore, RDD is readily applied to $R_{1\rho}$ dispersion (Korzhnev et al. 2005) and other spin-types of R_2 dispersion experiments such as $^1H^N$, $^1H^\alpha$, $^{13}C^\alpha$, and ^{13}CO (Korzhnev and Kay 2008) because RDD requires no modification of their pulse programs. In addition, subtracted RD spectra are used for confirming some of the signal assignments that are performed in a regular manner in multi-dimensional NMR experiments. The residues sequentially adjacent to fluctuating residues commonly fluctuate together. In other words, a group of consecutive residues in a protein show relaxation dispersions, for example, the F helix in HO-1. Since the subtracted RD spectra contain only signals of fluctuating residues, the assignments of such signals including those that are overlapped with other signals in the unsubtracted spectra become more definite.

Since the RDD method requires multiple RD datasets measured with different T_{CPMG} delays, the total experimental time is longer than the regular RD experiment. Thus, the RDD method could be difficult to apply to unstable proteins whose NMR spectra should be measured in a short period of time. However, we recently developed a method to accelerate RD measurements with little loss in spectral resolution and accuracy of observed signal intensities by using nonuniform sampling (NUS) and a NUS-processing method called SIFT (Matsuki et al. 2011). This method can also be used for shortening the total experimental time needed to measure the multiple RD datasets required for the RDD method.

Recent improvements in stability of NMR spectrometers enable the easy application of the spectral subtraction technique to various NMR studies in order to remove background or unimportant signals, such as in interaction analyses using saturation transferred difference (STD)-NMR (Meyer and Peters 2003), in-cell NMR (Banci et al. 2013; Popovic et al. 2015), and metabolomics studies (Kikuchi et al. 2005). The signals left in substracted spectra can even be quantitatively analyzed. For examaple, dissociation constants of ligand-receptor interactions are determined by STD-NMR experiments (Angulo and Nieto 2011). Our results demonstrate that signal intensities in the subtracted RD spectra can also be analyzed quantitatively by the RDD method. Thus, our study expands the range of applications of the spectral subtraction technique. However, it should be noted that signals of fluctuating residues must be separated from those of other fluctuating residues for the RDD method. Therefore, chemical shifts of overlapped signals that are assigned by multi-dimensional NMR experiments should be carefully checked. Furthermore, signals remaining in the subtracted spectra should be examined by checking the RD profiles of the residues adjacent to the ones whose signals are overlapped. The RD profiles are obtained by processing one of the datasets measured for the RDD method in a regular RD experiment manner.

In summary, we have developed relaxation dispersion difference, RDD, which is a novel methodology for analyzing overlapped signals in RD experiments with neither selective isotope labeling nor modification of the pulse programs. Using RDD, we extracted dynamics information of free HO-1 from overlapped signals that were previously unable to be processed by the conventional RD method. RDD can be widely applied to elucidate the dynamics of proteins and any other molecule that is amenable to the RD measurement.

Acknowledgments This work was supported by a Grant-in-Aid for Scientific Research on Innovative Areas for K. S. and a Grant-in-Aid for Young Scientists (B) for T. K. from the MEXT of Japan.

References

Angulo J, Nieto PM (2011) STD-NMR: application to transient interactions between biomolecules—a quantitative approach. Eur Biophys J 40:1357–1369

Banci L, Barbieri L, Bertini I, Luchinat E, Secci E, Zhao Y, Aricescu AR (2013) Atomic-resolution monitoring of protein maturation in live human cells by NMR. Nat Chem Biol 9:297–299

Bhabha G, Lee J, Ekiert DC, Gam J, Wilson IA, Dyson HJ, Benkovic SJ, Wright PE (2011) A dynamic knockout reveals that conformational fluctuations influence the chemical step of enzyme catalysis. Science 332:234–238

Boehr DD, Dyson HJ, Wright PE (2006a) An NMR perspective on enzyme dynamics. Chem Rev 106:3055–3079

Boehr DD, McElheny D, Dyson HJ, Wright PE (2006b) The dynamic energy landscape of dihydrofolate reductase catalysis. Science 313:1638–1642

Carver JP, Richards RE (1972) A general two-site solution for the chemical exchange produced dependence of T2 upon the Carr–Pursell pulse separation. J Magn Reson 6:89–105

Delaglio F, Grzesiek S, Vuister GW, Zhu G, Pfeifer J, Bax A (1995) NMRPipe: a multidimensional spectral processing system based on UNIX pipes. J Biomol NMR 6:277–293

Gutmanas A, Tu L, Orekhov VY, Billeter M (2004) Accurate relaxation parameters for large proteins. J Magn Reson 167:107–113

Harada E, Sugishima M, Harada J, Noguchi M, Fukuyama K, Sugase K (2015a) Backbone assignments of the apo and Zn(II) protoporphyrin IX-bound states of the soluble form of rat heme oxygenase-1. Biomol NMR Assign 9:197–200

Harada E, Sugishima M, Harada J, Noguchi M, Fukuyama K, Sugase K (2015b) Regulation of substrate-binding by a hidden distal effect via intrinsic fluctuation. Biochemistry 53:340–348

Henzler-Wildman KA, Thai V, Lei M, Ott M, Wolf-Watz M, Fenn T, Pozharski E, Wilson MA, Petsko GA, Karplus M, Hubner CG, Kern D (2007) Intrinsic motions along an enzymatic reaction trajectory. Nature 450:838–844

Johnson BA, Blevins RA (1994) NMR view: a computer program for the visualization and analysis of NMR data. J Biomol NMR 4:603–614

Kikuchi G, Yoshida T, Noguchi M (2005) Heme oxygenase and heme degradation. Biochem Biophys Res Commun 338:558–567

Korzhnev DM, Kay LE (2008) Probing invisible, low-populated States of protein molecules by relaxation dispersion NMR spectroscopy: an application to protein folding. Acc Chem Res 41:442–451

Korzhnev DM, Orekhov VY, Kay LE (2005) Off-resonance R(1rho) NMR studies of exchange dynamics in proteins with low spin-lock fields: an application to a Fyn SH3 domain. J Am Chem Soc 127:713–721

Lad L, Schuller DJ, Shimizu H, Friedman J, Li H, Ortiz de Montellano PR, Poulos TL (2003) Comparison of the heme-free and -bound crystal structures of human heme oxygenase-1. J Biol Chem 278:7834–7843

Lightning LK, Huang H, Moenne-Loccoz P, Loehr TM, Schuller DJ, Poulos TL, de Montellano PR (2001) Disruption of an active site hydrogen bond converts human heme oxygenase-1 into a peroxidase. J Biol Chem 276:10612–10619

Liu Y, Koenigs Lightning L, Huang H, Moenne-Loccoz P, Schuller DJ, Poulos TL, Loehr TM, Ortiz de Montellano PR (2000) Replacement of the distal glycine 139 transforms human heme oxygenase-1 into a peroxidase. J Biol Chem 275:34501–34507

Loria JP, Rance M, Palmer AG (1999a) A relaxation-compensated Carr–Purcell–Meiboom–Gill sequence for characterizing chemical exchange by NMR spectroscopy. J Am Chem Soc 121:2331–2332

Loria JP, Rance M, Palmer AG 3rd (1999b) A TROSY CPMG sequence for characterizing chemical exchange in large proteins. J Biomol NMR 15:151–155

Matsuki Y, Konuma T, Fujiwara T, Sugase K (2011) Boosting protein dynamics studies using quantitative nonuniform sampling NMR spectroscopy. J Phys Chem B 115:13740–13745

Meinhold DW, Wright PE (2011) Measurement of protein unfolding/refolding kinetics and structural characterization of hidden intermediates by NMR relaxation dispersion. Proc Natl Acad Sci USA 108:9078–9083

Meyer B, Peters T (2003) NMR spectroscopy techniques for screening and identifying ligand binding to protein receptors. Angew Chem Int Ed Engl 42:864–890

Nashine VC, Hammes-Schiffer S, Benkovic SJ (2010) Coupled motions in enzyme catalysis. Curr Opin Chem Biol 14:644–651

Popovic M, Sanfelice D, Pastore C, Prischi F, Temussi PA, Pastore A (2015) Selective observation of the disordered import signal of a globular protein by in-cell NMR: the example of frataxins. Protein Sci 4:996–1003

Sugase K, Dyson HJ, Wright PE (2007a) Mechanism of coupled folding and binding of an intrinsically disordered protein. Nature 447:1021–1025

Sugase K, Lansing JC, Dyson HJ, Wright PE (2007b) Tailoring relaxation dispersion experiments for fast-associating protein complexes. J Am Chem Soc 129:13406–13407

Sugase K, Konuma T, Lansing JC, Wright PE (2013) Fast and accurate fitting of relaxation dispersion data using the flexible software package GLOVE. J Biomol NMR 56:275–283

Tollinger M, Skrynnikov NR, Mulder FA, Forman-Kay JD, Kay LE (2001) Slow dynamics in folded and unfolded states of an SH3 domain. J Am Chem Soc 123:11341–11352

Tugarinov V, Choy WY, Kupce E, Kay LE (2004) Addressing the overlap problem in the quantitative analysis of two dimensional NMR spectra: application to (15)N relaxation measurements. J Biomol NMR 30:347–352

Vallurupalli P, Hansen DF, Kay LE (2008) Structures of invisible, excited protein states by relaxation dispersion NMR spectroscopy. Proc Natl Acad Sci USA 105:11766–11771